Journal of the European Optical Society - Rapid Publications 1, 06031 (2006) www.jeos.org

Inversion of a guided optical vortex

A. V. Carpentier Área de Óptica, Facultade de Ciencias de Ourense, Universidade de Vigo, As Lagoas s/n, Ourense, ES-32004 Spain.

H. Michinel Área de Óptica, Facultade de Ciencias de Ourense, Universidade de Vigo, As Lagoas s/n, Ourense, ES-32004 Spain.

J. R. Salgueiro Área de Óptica, Facultade de Ciencias de Ourense, Universidade de Vigo, As Lagoas s/n, Ourense, ES-32004 Spain.

S. Doval Área de Óptica, Facultade de Ciencias de Ourense, Universidade de Vigo, As Lagoas s/n, Ourense, ES-32004 Spain.

A. Ferrando Área de Óptica, Facultade de Ciencias de Ourense, Universidade de Vigo, As Lagoas s/n, Ourense, ES-32004 Spain.

We demonstrate, both theoretically and experimentally, the inversion of the topological charge of a vortex that propagates through an optical fiber. In our experiment, we couple the vortex to a two-mode fiber and we control the charge inversion by deformation of the optical fiber.

Keywords: Optical vortices, charge inversion, fiber propagation

1 Introduction

In a light beam, a vortex is a screw dislocation in the field [1] around which the phase of the optical wave has an integer number of windings l, a quantity which is usually called topological charge of the singularity. Optical vortices have attracted much attention in recent years, due to its fundamental importance as topological objects and also to their applications in particle trapping [2], waveguiding [3] or transmission of angular momentum to neutral particles [4]. Technological applications like the recently developed *optical vortex coronagraph* [5] used in optical search of planets or *optical tweezers* [6] that can exert torques on microscopic particles are based on different properties of optical vortices [7].

This kind of phase singularities in light beams can appear spontaneously due to the pass of a beam through a turbulent medium [8]. They can be generated by directly manipulating the optical resonator of a laser [9], or by the employment of a holographic mask [10]. Once produced, the phase singularity is highly stable and is only destroyed by annihilation with another vortex of opposite charge. Charge flipping of an optical vortex has been achieved by parametric frequency conversion [11]. In free space it has been shown that a cylindrical lens can be used to invert the vortex spin [12]. The ability to control the charge flipping allows to perform arithmetic operations with vortices [13] as well as to modify their angular momentum transfer and trapping properties.

In this Letter, we will show both theoretically and experimentally that it is possible to achieve and control the inversion of a guided vortex that propagates in an optical fiber. To this aim, we have employed a simple technique previously described in Ref. [14]. In this work the authors used a deformation of an optical fiber to convert a Hermite-Gaussian mode of the optical waveguide into a Laguerre-Gaussian mode with azimuthal variation of the phase. In our case, we launch at the input face of a bimode fiber [15, 16] a beam carrying an optical vortex with topological charge $l = 1$. Thus, the beam is coupled to one azimuthal mode of the waveguide and propagates until it reaches a zone where a slight deformation is applied to the fiber. The change in the radial profile yields to a rapid inversion of the vortex which is monitored at the output face of the waveguide, where it appears a vortex with $l = -1$.

The experiment is sketched in Figure 1. This allows a robust control of the charge flipping and simultaneously the guiding of the beam. This effects could have potential applications in the design of new types of optical tweezers that are able to induce variable torques in microscopic objects.

Thus, in first place we will present a theory based on the Poincare sphere and symmetry considerations, that allows to study analytically the problem of charge inversion. An equivalent theory is developed in Ref. [17]. We will check the va-

Received December 04, 2006; published December 18, 2006 ISSN 1990-2573

lidity of our analysis by numerical simulations and finally we will present the experimental results.

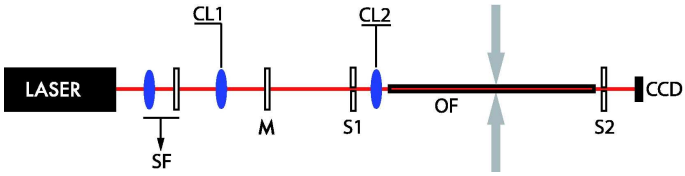

FIG. 1 Experimental setup: LASER: $4mW$ single frequency argon ion laser ($\lambda = 458nm$); SF: spatial filter composed by a microscopic lens and a pin hole; CL1: collimating lens; M: computer generated holographic mask; S1: adjustable slit or iris diaphragm; CL2: coupling lens; OF: optical fiber ($\lambda_c = 550nm$, $NA = 0.10 - 0.14$); S2: adjustable slit; CCD: camera for detecting the far field output of the fiber.

2 THEORY AND NUMERICAL SIMULATIONS

Evolution of a cw light beam in an axially z-invariant guiding medium (in the weakly guiding approximation) is given by the eigenmodes of the transverse operator $L \equiv \nabla_t^2 + k_0^2 n^2(\mathbf{x}_t)$; i.e., by eigenfunctions fulfilling $L\phi = \beta^2\phi$, β being the mode propagation constant. In a full rotational invariant medium, in which the refractive index depends on the radial coordinate only $n = n(r)$, modes are classified according to their angular momentum l and they appear in degenerated doublets of the type $\phi_l(r,\theta) = f_l(r)e^{\pm il\theta}$ corresponding to vortex-antivortex pairs. However, if we introduce some breaking of the original rotational symmetry, e.g., by means of an external action, mode degeneracy disappears according to strict rules determined by symmetry. Let us consider here that the external perturbation of the refractive index induces a breaking of the original symmetry. In such a case every originally degenerated doublet of angular momentum l splits into two non-degenerated eigenmodes ϕ_l^s and ϕ_l^a. At first-order degenerated perturbation theory these eigenmodes are given by the symmetric and antisymmetric combinations of angular momentum modes $\phi_l^s = \phi_l + \phi_l^*$ and $\phi_l^a = -(\phi_l - \phi_l^*)$. These combinations belong to the four one-dimensional representations of the $\mathcal{C}_{2v}$ group [18]. We consider that we properly illuminate the system in such a way there is no simultaneous excitation of more than one broken doublet. This is the case if we illuminate the system with a vortex carrying vorticity l, since then the projection onto eigenmodes with different l would be zero. In this situation, evolution is provided by the two eigenmodes of the perturbed system, ϕ_l^s and ϕ_l^a, characterized by the same l than the impinging vortex. The propagation constants of these modes $\beta_l^a = \beta_l + \Delta\beta_l^a$ and $\beta_l^s = \beta_l + \Delta\beta_l^s$ (β_l being the propagation constant of the unperturbed vortex) determine the evolution in the perturbed medium since the propagating field will be a linear combination of these eigenmodes:

$$\varphi_l(\mathbf{x_t}, z) = \alpha_l^a \phi_l^a(\mathbf{x}_t, 0)\exp[i\beta_l^a z] + \alpha_l^s \phi_l^s(\mathbf{x}_t, 0)\exp[i\beta_l^s z]. \quad (1)$$

In terms of the unperturbed vortex and anti-vortex fields ϕ_l and ϕ_l^* we have:

$$\varphi_l(\mathbf{x_t}, z) = \alpha_+^l(z)\phi_l(\mathbf{x_t}, 0) + \alpha_-^l(z)\phi_l^*(\mathbf{x_t}, 0), \quad (2)$$

where

$$\alpha_\pm^l(z) \equiv \alpha_l^s \exp[i\beta_l^s z] \mp \alpha_l^a \exp[i\beta_l^a z]. \quad (3)$$

The initial values $\alpha_+^l(0)$ and $\alpha_-^l(0)$ are, by construction, the projections of the input amplitude onto the vortex and anti-vortex functions ϕ_l and ϕ_l^*. It is useful to write them in terms of the mixing angle θ as $\alpha_+^l(0) = \cos\theta$ and $\alpha_+^l(0) = \sin\theta$. Thus $\theta = 0$ means that we are taking as an initial state a vortex of charge l whereas $\theta = \pi/2$ means we are choosing an anti-vortex. Notice that the $(\alpha_+^l,\ \alpha_-^l)$ pair can be considered as a complex vector in which a vortex configuration is represented as the $(1,0)$ vector and an anti-vortex as the $(0,1)$ one. For this reason, the $(\alpha_+^l,\ \alpha_-^l)$ pair is formally identical to a Jones vector representing a polarization state. Because of this analogy, it is also very illustrative to use the alternative representation of polarization in terms of a Stokes vector. The evolution of the complex Jones vector in z is then visualized as a trajectory in the Poincaré sphere in which the north pole corresponds to a vortex configuration —$(1,0,0)$— and the south pole to an anti-vortex one —$(-1,0,0)$. The trajectory in the unit Poincaré sphere is given by ($\Delta\beta_l \equiv \beta_a^l - \beta_s^l$):

$$\begin{aligned} S_1(z) &= \cos 2\theta \cos[\Delta\beta_l z], \\ S_2(z) &= -\cos 2\theta \sin[\Delta\beta_l z], \\ S_3(z) &= \sin 2\theta. \end{aligned}$$

We can see that if the initial condition is given by an input vortex —$\theta = 0$—, the trajectory becomes a circle on a meridian characterized by $S_3 = 0$ (i.e., in the S_1-S_2 plane) and the motion is periodic with period given by $L = 2\pi/\Delta\beta_l$. The motion certainly shows charge inversion since the vortex mutes into an anti-vortex and vice-versa every $L/2 = \pi/\Delta\beta_l$.

In order to check the validity of the theoretical analysis, we have simulated the propagation of an input Gaussian beam with a nested vortex through an optical fiber that is deformed at some point into a $\mathcal{C}_{2v}$ structure. The results are shown in Figure 2.

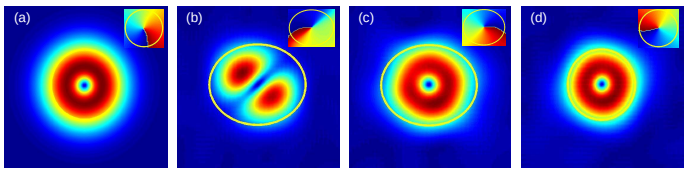

FIG. 2 Numerical simulation showing the propagation of a Gaussian beam with a nested vortex with charge $l = 1$ through an optical fiber that is deformed at some point. The yellow line indicates the boundary of the fiber. Insets display the phase distribution. The false color image in a) displays the intensity distribution of the input beam ; b) and c) show the vortex inversion due to deformation of the fiber; d) corresponds to the output vortex with flipped charge.

To simulate the evolution of an input beam with topological charge one (Figure 2a), we have used a split-step Fourier method in a grid of 512×512 points, with a step in propagation of the order of the wavelength λ. The pictures are false-color contours of the intensity in the plane transverse to propagation.

As it can be appreciated in the pictures, the input beam propagates without distortion until it reaches the zone where the fiber is deformed (the yellow line indicates the boundary of the fiber core). In the region where the fiber takes a elliptical shape, the degeneracy is broken and the vortex excites a dipole with a 45^o node, which finally evolves into a vortex with opposite charge (insets display phase distribution). Once the fiber recovers the circular shape, the new vortex state is preserved. The effect of the deformation is to accelerate the inversion of the vortex, i.e.: the higher the deformation of the fiber, the quicker the inversion. Thus, the region over which the fiber is deformed, is sensibly reduced by increasing the ellipticity of the cross section of the fiber. This can be appreciated in Figure 3 where we plot the results from numerical simulations for different eccentricities of the fiber core. The horizontal axis represents $\epsilon = \sqrt{1 - r_y^2/r_x^2}$, being r_x and r_y the radius of the elliptical core along x and y respectively. The vertical axis shows the distance for vortex inversion inside the fiber used in experiments with cutoff wavelength $550nm$ and core radius $5\mu m$. The laser wavelength is $458nm$.

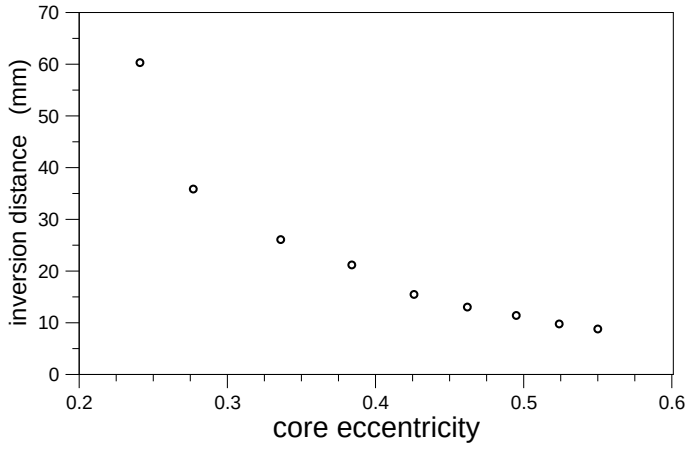

FIG. 3 Results from numerical simulations for different eccentricities of the fiber core. The horizontal axis represents $\epsilon = \sqrt{1 - r_y^2/r_x^2}$, being r_x and r_y the radius of the elliptical core along x and y respectively. The vertical axis shows the distance for vortex inversion inside the fiber used in experiments with cutoff wavelength $550nm$ and core radius $5\mu m$. The laser wavelength is $458nm$.

3 EXPERIMENTAL RESULTS

A sketch of the experimental setup is shown in Figure 1. We have used a $4mW$ Argon Ion laser with an output wavelength $\lambda = 458nm$, a computer generated holographic mask of topological charge $l = 1$ [10], and an optic fiber with a cut-off wavelength $\lambda_c = 550nm$ and a numerical aperture $NA = 0.10 - 0.14$. This fiber has two modes at the laser wavelength: the fundamental and the first excited one (which is degenerated) allowing the coupling of the vortex mode. We first clean the beam with a spatial filter composed by a lens and a pin hole at the focus length (SF in the figure). After collimating the beam (CL1), it traverses the holographic mask (M) forming a diffraction pattern. We separate the first diffracted order by an adjustable iris diaphragm (S1) obtaining an optical vortex with topological charge $l = 1$. The optical vortex is then coupled to the optic fiber (OF) by focusing it to the input face with a microscope objective lens (CL2). We visualize the fiber output by monitoring it with a charge-coupled device (CCD) camera. For detecting the phase profile, we introduce between the end of the fiber and the CCD an adjustable slit (S2) which produces border diffraction, creating the characteristic fork pattern.

Images of the experiment showing the optical vortex before and after propagation along the optical fiber are displayed in Figure 4. The intensity profiles obtained from the photography show the characteristic zone of null intensity let in the center of the light field. It is interesting to notice the filtering effect of the bimode fiber that cleans the optical field eliminating a great part of the input noise.

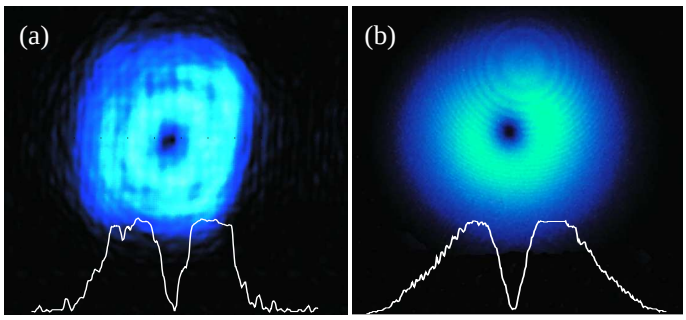

FIG. 4 Far field intensity image of the optical vortex registered with the CCD camera before (a) and after (b) the propagation through the optical fiber. White lines are the intensity profiles across the center of the vortex.

In Figure 5 we can see the intensity and phase profiles before (a) during (b) and after (c) the deformation of the fiber. The deformation was applied by pressing the fiber with a screw. The method is very simple and robust. We must stress that faster techniques like electrooptic modulators could be used in order to produce the same effect. To visualize the characteristic fork pattern of the interference of a vortex with a tilted planar wave, we simply approximate the edge of a linear slit to the border of the beam. Thus, the part of the beam diffracted by the border interferes with the vortex field, resulting in the series of images in the right hand of Figure 5.

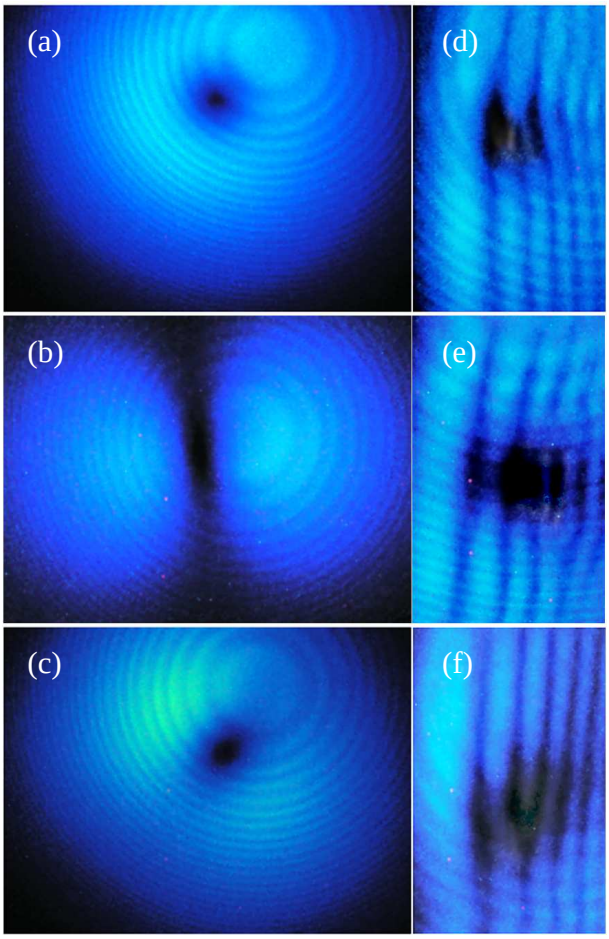

FIG. 5 Intensity profiles of the optical vortex at the output of the fiber before (a), during (b) and after (c) deformation. (d), (e) and (f) are their respective phase profiles showing the inversion of the output vortex.

In the movie (Click to watch the movie Fig6.mov for Figure 6) we can see the phase profile at the output of the optical fiber while it was deformed. The variation of the fork pattern prove that the topological charge of the vortex is inverted.

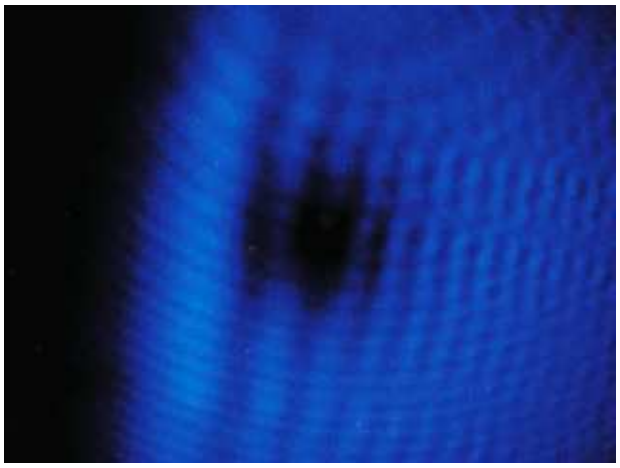

FIG. 6 Movie showing the phase pattern of four inversions of the optical vortex that were induced by deforming the optical fiber. (Format: QuickTime. Size: $4.8Mb$)

4 CONCLUSIONS

We have demonstrated both theoretically and experimentally the coupling of an optical vortex of topological charge $l = 1$ to an optic fiber, and the inversion of the topological charge of the vortex inside the guide by producing a deformation of the fiber section. This process could have potential applications in the design of novel types of tweezers of variable transfer of momentum, faster processes based on electrooptic effects that change the effective index in a limited region of the fiber could also be used to achieve the same charge flipping effect and the simultaneous guiding of the vortex.

ACKNOWLEDGMENTS

This work was supported by Ministerio de Educación y Ciencia, Spain (projects FIS2004-02466, FIS2005-01189, BFM2003-02832, network FIS2004-20188-E), Xunta de Galicia (project PGIDIT04TIC383001PR). JRS acknowledges a Ramón y Cajal Contract granted by the Secretaría de Universidades e Investigación of Spain.

References

[1] J. F. Nye and M. V. Berry, "Dislocations in wave trains" Proc. R. Soc. London Ser. A **336**, 165-190 (1974).

[2] H. He, M. E. J. Friese, N. R. Heckenberg, and H. Rubinsztein-Dunlop, "Direct observation of transfer of angular-momentum to absorptive particles from a laser-beam with a phase singularity" Phys. Rev. Lett. **75**, 826-829 (1995).

[3] A. H. Carlsson, J. N. Malmberg, D. Anderson, M. Lisak, E. A. Ostrovskaya, T. J. Alexander, and Y. S. Kivshar, "Linear and nonlinear waveguides induced by optical vortex solitons" Opt. Lett. **25**, 660-662 (2000).

[4] N. B. Simpson, K. Dholakia, L. Allen, and M. J. Padgett, "Mechanical equivalence of spin and orbital angular momentum of light: An optical spanner" Opt. Lett. **22**, 52-54 (1997).

[5] G. Foo, D. M. Palacios, and G. A. Swartzlander, Jr., "Optical vortex coronagraph" Opt. Lett. **30**, 3308-3310 (2005).

[6] K. T. Gahagan, and G. A. Swartzlander, Jr., "Optical vortex trapping of particles" Opt. Lett. **21**, 827-829 (1996).

[7] M. Vasnetsov and K. Staliunas Eds., *Optical Vortices*, Nova Science, New York (1999).

[8] N. B. Baranova, A. V. Mamaev, N. F. Pilipetsky, N. F. Shkunov, and V. V. Zeldovich, "Wave-front dislocations. Topological limitations for adaptive systems with phase conjugation" J. Opt. Soc. Am. **73**, 525-528 (1983).

[9] P. Coullet, L. Gil, and F. Rocca, "Optical vortices" Opt. Comm. **73**, 403-408 (1989).

[10] N. R. Heckenbeerg, R. McDuff, C. P. Smith, and A. G. White, "Generation of optical-phase singularities by computer-generated holograms" Opt. Lett. **17**, 221-223 (1992).

[11] A. Berzanskis, A. Matijosius, A. Piskarskas, V. Smilgevicius, and A. Stabinis, "Conversion of topological charge of optical vortices in a parametric frequency converter" Opt. Co. **140**, 273-276 (1997).

[12] G. Molina-Terriza, J. Recolons, J. P. Torres, and Lluis Torner "Observation of the dynamical inversion of the topological charge of an optical vortex" Phys. Rev. Lett. **87**, 023902 (2001).

[13] G. Molina-Terriza, J. Recolons, and L. Torner, "The curious arithmetic of optical vortices" Opt. Lett. **25**, 1135-1137 (2000).

[14] D. McGloin, N. B. Simpson, and M. J. Padgett, "Transfer of orbital angular momentum from a stressed fiber-optic waveguide to a light beam" Appl. Opt. **37**, 469-472 (1998).

[15] A. V. Volyar,and T. A. Fadeeva, "Vortical nature of optical-fiber modes. IV. Orthogonal transformations of topological charge and circular polarization of an optical vortex" Tech. Phys. Lett. **22**, 722-724 (1996).

[16] A. N. Alexeyev, T. A. Fadeeva, A. V. Volyar, and M. S. Soskin, "Optical vortices and the flow of their angular momentum in a multimode fiber" Sem. Cond. Phys., Quant. Elect. and Opt. **1**, 82-89 (1998).

[17] M. J. Padgett, and J. Courtial, "Poincaré-sphere equivalent for light beams containing orbital angular momentum" Opt. Lett. **24**, 430-432 (1999).

[18] M. Hamermesh, *Group theory and its application to physical problems* (Addison-Wesley, Reading, Massachusetts 1964).